

Role of Relative Transition Energy Level in Regioselective Chlorinations on Bithiophenes: Ab Initio Study

Yong-Jin Yoon,[1] In Sun Koo,[2] and Jong Keun Park*[2]

[1]Department of Chemistry, Research Institute of Natural Science, Graduate School for Materials and Nanochemistry, Gyeongsang National University, Jinju 660-701, Korea

[2]Department of Chemistry Education and Research Institute of Natural Science, Educational Research Institute Teachers College, Gyeongsang National University, Jinju 660-701, Korea

Received June 22, 2010; E-mail: mc7@gnu.ac.kr

The equilibrium and transition geometric structures from bithiophene to hexachlorobithiophene derivatives and relative energies of bithiophene derivatives in electrophilic chlorination were fully optimized using the ab initio Hartree–Fock and second-order Møller–Plesset perturbation method with a 6-311+G** basis set. The regioselectivity of the electrophilic chlorination of bithiophene derivatives was determined primarily by the gaps (ΔE_1, ΔE_2, ΔE_3, ...) of the relative transition energy levels in the transition π-complexes. The gaps of the relative transition energy level were correlated with both the chlorinated positions and atomic charges of the carbon atoms on the bithiophene ring, the HOMO–LUMO gaps of the transition π-complexes due to the ($Cl^{+}\cdots C^{\delta-}$) interaction, the geometric structures of the neutral and transition derivatives, and the π-conjugation effect (delocalization energy) originating from the π-orbitals. The order of relative stability in the transition π-complexes was found to be 5,5′-dichlorinated > 3,3′-dichlorinated > 4,4′-dichlorinated derivatives. Particularly, with increasing the relative transition energy gaps (ΔE_2, ΔE_3, ΔE_8, ΔE_9, ...) in the transition π-complexes, the regioselective chlorinations from **BT** to **6Cl-BT** occurred at specific position of bithiophenes.

Oligo- and polythiophene derivatives have been intensively researched as materials with numerous potential uses as flexible displays, electronic cards, sensors, and in other applications. These derivatives show conductive, magnetic, nonlinear optical, electroluminescence, and electrofluorescence properties.[1–6] These properties are influenced by the low-band energy gap originating from the effects of π-conjugation. Because of these versatile properties, derivatives with the lowest band gap have been elegantly designed and selectively synthesized by several theoretical[7–9] and experimental[10–13] groups. To synthesize bithiophene derivatives with these functional properties, a special functional moiety is bonded to a specific position of the derivatives. Halo-substituted 2,2′-bithiophene is a common starting precursor used to synthesize polythiophenes with special moieties (The halogenation of 2,2′-bithiophene provides a low potential oxidation energy compared to that of thiophene.).[14] Regioselective halogenations of 2,2′-bithiophene are performed using either coupling reactions[10–14] or other standard methods[15–17] described in the literature. The selective substitution at specific positions of bithiophene derivatives is an important step in the preparation of well-defined oligothiophenes.[10–17]

In the transition-metal-catalyzed coupling reactions of bithiophene derivatives, 5,5′-substituted bithiophene intermediates were regioselectively formed via electrophilic C_5–H substitutions.[10–13] Particularly, in the halogenation of 2,2′-bithiophenes,[15–17] four types of chlorobithiophenes (5-chloro-, 5,5′-dichloro-, 3,5,5′-trichloro-, and 3,3′,5,5′-tetrachlorobithiophene) were synthesized selectively. Penta- and hexachlorobithiophenes were not observed by the groups that utilized these methods. Meanwhile, other groups[18,19] reported the presence of the halogenated bithiophene derivatives. In the 2,2′-bithiophene derivatives, the electrophilic chlorination proceeds with high selectivity at the 5,5′-positions.[15–17] From dihalo- to tetrahalobithiophenes, the derivatives were subsequently synthesized. After the 5,5′-positions were substituted, the 3,3′-substituted derivatives were observed. The substitution reaction of halogen to 2,2′-bithiophene is experimentally favored at 5,5′-positions adjacent to sulfur compared to 3,3′- and 4,4′-positions.[7–15] Although research investigating the different selectivities (preferred position, specific reactivity, etc.) have been performed using both theoretical[7–9] and experimental[10–19] approaches, the driving forces controlling this regioselectivity are not yet well understood.

What is the driving force for the regioselectivity in electrophilic substitutions of the bithiophene derivatives? The selective halogenations of bithiophenes using 2-halopyridazin-3(2*H*)-ones under catalyzed transition metal conditions were very recently suggested by Jung et al.,[17] 5,5′-dihalo-, 3,5,5′-trihalo-, and 3,3′,5,5′-tetrahalobithiophenes were synthesized selectively and sequentially. In the halogenations of bithiophenes using transition-metal-catalyzed coupling reactions performed by Sone and Abe, the chlorination occurs preferentially at the 5,5′-positions and sequentially at the 3,3′-positions on the derivatives.[16] In the electrophilic brominations of bithiophenes investigated by Kellogg et al.,[15] the reaction under the brominating agent *N*-bromosuccinimide in mixed chloroform–acetic acid proceeded with high selectivity in the

Published on the web February 4, 2011; doi:10.1246/bcsj.20100167

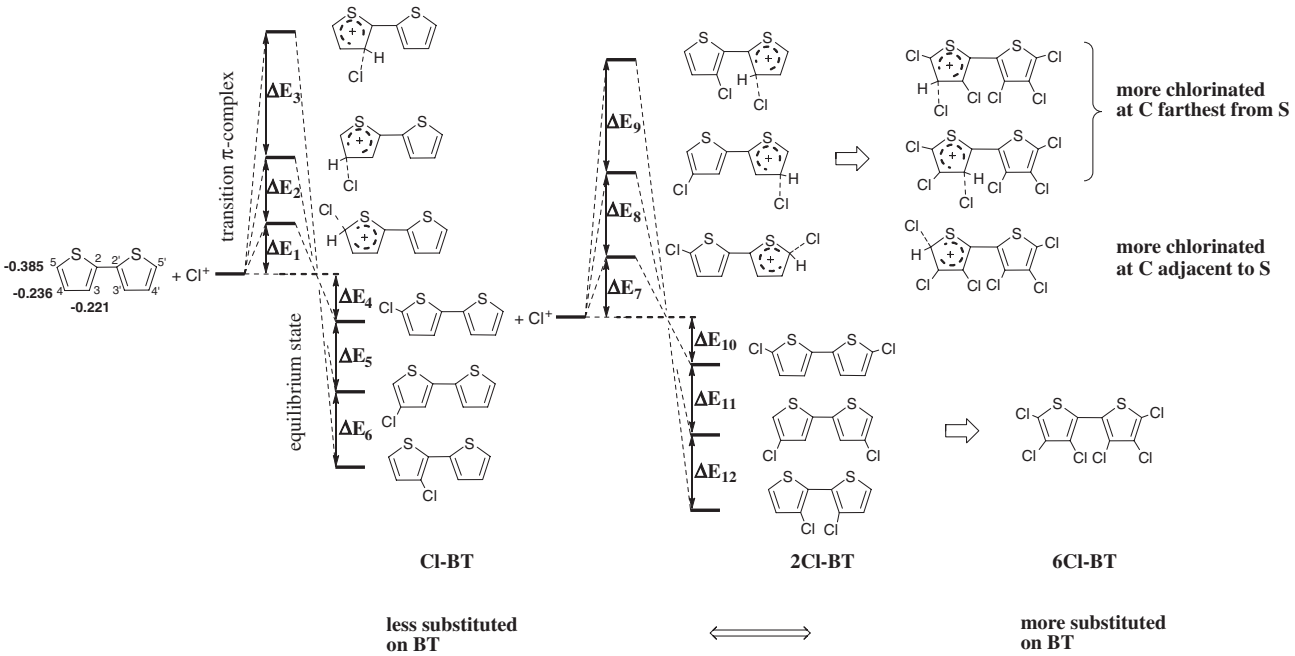

Scheme 1. Schematic diagram for the sequentially electrophilic chlorination at the specific 5,5′- (4,4′-, 3,3′-)carbons on 2,2′-bithiophene derivatives.

5,5′-positions. Legault et al.[20,21] recently suggested that two factors that control the selectivity of palladium-catalyzed halogenations originate from both the bond dissociation energy and the HOMO–LUMO interaction between Pd and heterocycles. Although that previous study explained the sequential mechanism of the two steps for the regioselectivity, the origin of the selectivity at the specific position remains unknown. Some groups experimentally investigated the order and site predictions for coupling reactions in polyhaloheteroaromatics using NMR spectroscopy.[22,23] Using NMR, the changed environments of the carbon atom bonded by different substituents were described by the chemical shift differences. Using the delocalization of the Wheland intermediates, the regioselectivity for the electrophilic halogenation of thiophene was explained by Joule et al.[24] The π-complex substituted at the 5-position of thiophene was found to be stabilized by the resonance contribution. However, in the case of the selectivity for the order and the specific position, the preferred source governing the selectivity has not yet been described.

Although some studies suggested that several factors (including C–X bond strength, bond dissociation energy, orbital interaction, etc.) influence the selectivity of halogenation reactions, the selective reactions on bithiophene derivatives may be basically dependent on the relative transition energy gap ($\Delta E_{\text{transition}}$) of transition π-complexes in the rate-determining step. The energy level of transition π-complexes with high selectivity may be mainly related to both the position and strength of the ($Cl^{\delta+}\cdots C^{\delta-}$) interaction, the relative stability added by the π-conjugation effect of the aromatic ring, and the geometric structures (structural parameters of $R_{C2-C2'}$ and ϕ, steric hindrance) between two thiophene rings. To investigate the origins (detailed factors) for the regioselectivity, the schematic diagram for the sequential chlorination on bithiophene derivatives was presented in Scheme 1.

We were interested in the high selectivity of the bithiophene chlorinations, which allowed us to investigate the driving forces (in both the preferred source and origin) for the electrophilic substitution of chlorine. We first optimized the equilibrium and transition structures of the chlorobithiophene derivatives. The geometric structures for equilibrium and transition conformers and the reaction energy profiles for the binding between chlorine and bithiophene were analyzed. As shown in Scheme 1, the sources of the selectivity were predicted both qualitatively and quantitatively. Computational results gave further information for the selectivity. A thorough understanding of the selective chlorinations of bithiophenes will provide the basis for determining characteristic factors associated with this product, including conformation and relative stability, and will produce an efficient sequential preparation procedure.

Computational Methods

The neutral and transition structures from bithiophene to hexachlorobithiophene derivatives were fully optimized with the Hartree–Fock (HF) and second-order Møller–Plesset (MP2)/6-311+G** levels using Gaussian 03.[25] To investigate the reactive mechanism for the electrophilic chlorination of the bithiophene derivatives, all possible geometric structures including the *anti*- and *syn*-types were calculated. The relative potential energies of the equilibrium and transition conformers were evaluated, and the relative energy profiles for the binding between chlorine and bithiophene derivatives were analyzed. The relative potential energy diagrams including the reactants, the transition π-complexes, and the products were produced using the MP2 results. Furthermore, the atomic charges of the natural bond orbital (NBO) of the derivatives were investigated. To confirm the existence of stable structures, the harmonic vibrational frequencies of the species were analyzed

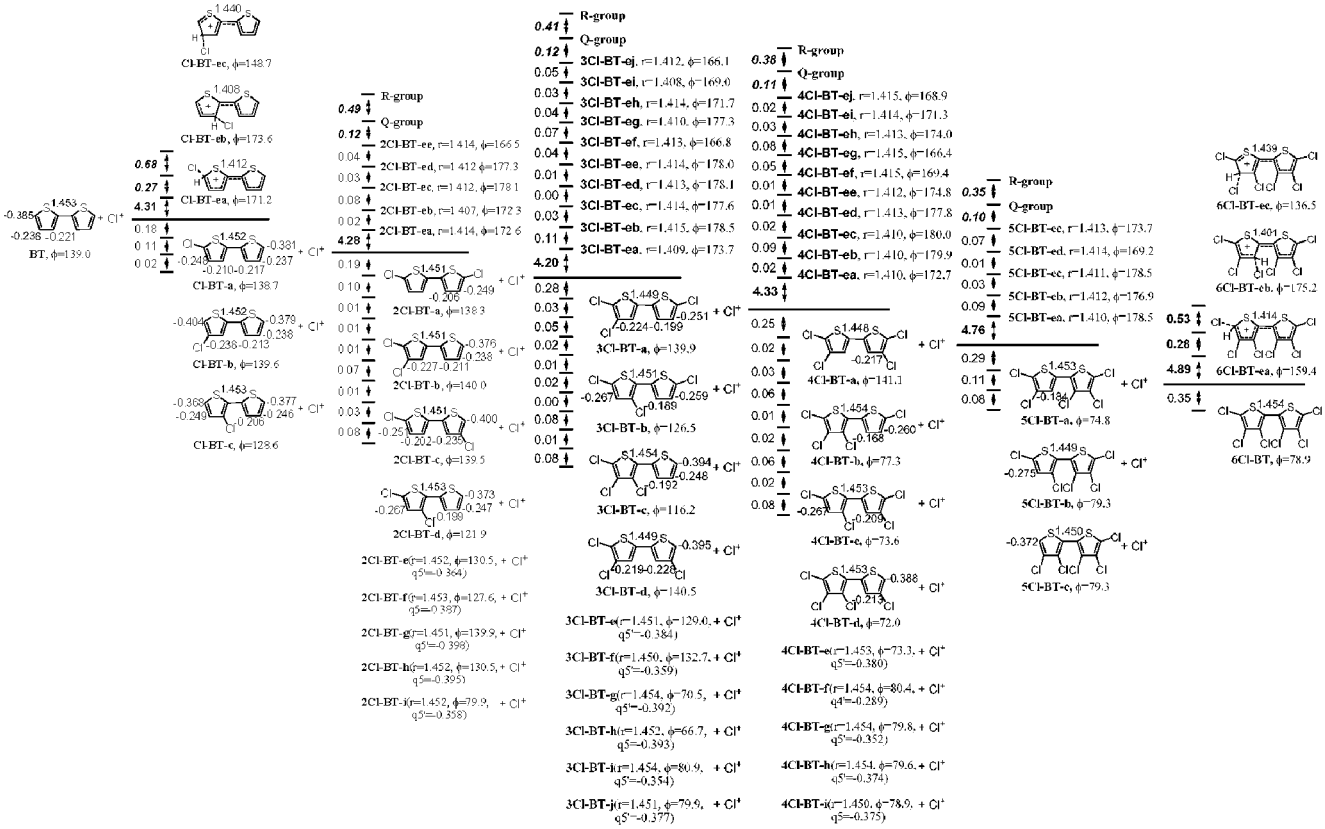

Figure 1. *Continued on the next page.*

at the level of HF/6-311+G**. The frequencies of the bithiophene derivatives were all positive signs.

Results and Discussion

All possible geometric structures of the equilibrium and transition derivatives were optimized at the MP2/6-311+G** level and the relative potential energy diagrams including the geometric parameters and the atomic charges are presented in Figure 1. In the neutral derivatives, the geometric structures display two local energy minima ranging from $\phi = 0.0$ to 180.0 degrees ($\phi \approx 65$–80 degrees for pseudo-*syn*-type and $\phi \approx 116$–140 degrees for pseudo-*anti*). In each chlorination step from **BT** to **6Cl-BT**, the 5,5′-dichlorinated neutral derivatives (the more chlorinated at the C adjacent to the S) were more unstable than 3,3′- and 4,4′-dichlorinated derivatives (more chlorinated at the C farthest from S). That is, in the chlorination step, the relative transition energy gaps (ΔE_1, ΔE_7, ...) from 5,5′-dichlorinated neutrals to transition π-complexes was smaller than those of the others. By the smallest energy gaps, the 5,5′-dichlorinated neutrals easily varied to transition π-complexes. As a result, each chlorination on the bithiophenes proceeded to be energetically favored at the specific 5,5′-positions.

From **BT** to **3Cl-BT-f** including **4Cl-BT-a**, except for **2Cl-BT-i** (less substituted at the C), the pseudo-*anti* was more stable than pseudo-*syn* (Figure 1). The electronegative S and Cl atoms adopted electron-withdrawing characteristics. The π-electron density on the ring became localized to the S and Cl atoms. By the repulsion of (S···S), the relative energy of the pseudo-*anti* was lower than that of the pseudo-*syn*. Meanwhile, from **3Cl-BT-g** to **6Cl-BT** including **2Cl-BT-i**, except for **4Cl-BT-a** (more substituted at the C), the neutral derivatives were automatically optimized to be vertical. When the Cl atom bound to the 3,3′-carbons, the (Cl···Cl) and (S···S) repulsions were induced by the electronegativity of Cl. The optimized structures of 3,3′-dichlorinated derivatives were found to be more perpendicular ($\phi \approx 79.9$ for **2Cl-BT-i**). With increasing the number of the chlorine, the $r_{C2-C2'}$ length and the dihedral angle of ϕ also increased. The geometric stabilities of the chlorinated neutral bithiophenes may be determined by the repulsions of (Cl···Cl) and (S···S) and the number and position of the substituted chlorine. In order to decrease the steric hindrance created by the chlorination, the geometric parameters ($r_{C2-C2'}$ and ϕ increased) were modified to reach a minimum conformation. These values were in good agreement with theoretical (1.451–1.465 Å)[26–30] and experimental (1.447–1.456 Å)[31,32] studies. As a result, our results for the geometry were similar to previous findings (with increasing the torsion angle, the π-conjugation decreases).[6–18,26–32] Particularly, these relative stabilities for the geometric conformations were in good agreement with the results reported by Bethmont et al.[33]

As shown in Figure 1, the structures of the transition π-complexes are classified by the chlorinated position and the relative energy level as three groups, namely 5,5′-dichlorinated (**P**), 3,3′-dichlorinated (**Q**), and 4,4′-dichlorinated (**R**) π-complexes. The relative energy level of **P** was the lowest. The energy gaps (0.52–0.68 eV) between **Q** and **R** were about two times those (0.27–0.50 eV) between **P** and **Q**. The relative energy gaps ($\Delta E_{\text{transition}} = 0.27$ eV) between **P** and **Q** at the first

P **Q** **R**

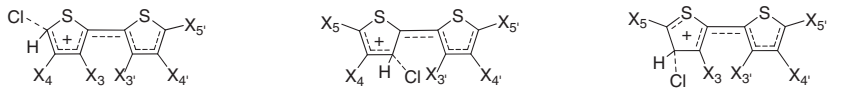

2Cl-BT-ea: X_4=Cl, X_3=$X_{3'}$=$X_{4'}$=$X_{5'}$=H
2Cl-BT-eb: $X_{5'}$=Cl, X_3=$X_{3'}$=X_4=$X_{4'}$=H
2Cl-BT-ec: $X_{3'}$=Cl, X_3=X_4=$X_{4'}$=$X_{5'}$=H
2Cl-BT-ed: $X_{4'}$=Cl, X_3=$X_{3'}$=X_4=$X_{5'}$=H
2Cl-BT-ee: X_3=Cl, $X_{3'}$=X_4=$X_{4'}$=$X_{5'}$=H

2Cl-BT-ef: $X_{3'}$=Cl, X_4=$X_{4'}$=X_5=$X_{5'}$=H
2Cl-BT-eg: $X_{5'}$=Cl, $X_{3'}$=X_4=$X_{4'}$=X_5=H
2Cl-BT-eh: X_4=Cl, $X_{3'}$=$X_{4'}$=X_5=$X_{5'}$=H
2Cl-BT-ei: $X_{4'}$=Cl, $X_{3'}$=X_4=X_5=$X_{5'}$=H
2Cl-BT-ej: X_5=Cl, $X_{3'}$=X_4=$X_{4'}$=$X_{5'}$=H

2Cl-BT-ek: X_3=Cl, $X_{3'}$=$X_{4'}$=X_5=$X_{5'}$=H
2Cl-BT-el: X_5=Cl, X_3=$X_{3'}$=$X_{4'}$=$X_{5'}$=H
2Cl-BT-em: $X_{3'}$=Cl, X_3=X_4=X_5=$X_{5'}$=H
2Cl-BT-en: $X_{4'}$=Cl, X_3=$X_{3'}$=X_5=$X_{5'}$=H
2Cl-BT-eo: $X_{5'}$=Cl, X_3=$X_{3'}$=$X_{4'}$=X_5=H

3Cl-BT-ea: X_4=$X_{5'}$=Cl, X_3=$X_{3'}$=$X_{4'}$=H
3Cl-BT-eb: $X_{3'}$=X_4=Cl, X_3=$X_{4'}$=$X_{5'}$=H
3Cl-BT-ec: X_4=$X_{4'}$=Cl, X_3=$X_{3'}$=$X_{5'}$=H
3Cl-BT-ed: $X_{3'}$=$X_{5'}$=Cl, X_3=X_4=$X_{4'}$=H
3Cl-BT-ee: $X_{3'}$=$X_{4'}$=Cl, X_3=X_4=$X_{5'}$=H
3Cl-BT-ef: X_3=X_4=Cl, $X_{3'}$=$X_{4'}$=$X_{5'}$=H
3Cl-BT-eg: $X_{4'}$=$X_{5'}$=Cl, X_3=$X_{3'}$=X_4=H
3Cl-BT-eh: X_3=$X_{3'}$=Cl, X_4=$X_{4'}$=$X_{5'}$=H
3Cl-BT-ei: X_3=$X_{5'}$=Cl, $X_{3'}$=X_4=$X_{4'}$=H
3Cl-BT-ej: X_3=$X_{4'}$=Cl, $X_{3'}$=X_4=$X_{5'}$=H

3Cl-BT-ek: $X_{3'}$=$X_{5'}$=Cl, X_4=$X_{4'}$=X_5=H
3Cl-BT-el: $X_{3'}$=X_4=Cl, $X_{4'}$=X_5=$X_{5'}$=H
3Cl-BT-em: X_3=$X_{4'}$=Cl, X_4=X_5=$X_{5'}$=H
3Cl-BT-en: $X_{3'}$=X_5=Cl, X_4=$X_{4'}$=$X_{5'}$=H
3Cl-BT-eo: X_4=$X_{5'}$=Cl, $X_{3'}$=$X_{4'}$=X_5=H
3Cl-BT-ep: $X_{4'}$=$X_{5'}$=Cl, X_3=X_4=X_5=H
3Cl-BT-eq: X_4=$X_{4'}$=Cl, $X_{3'}$=X_5=$X_{5'}$=H
3Cl-BT-er: X_4=X_5=Cl, $X_{3'}$=$X_{4'}$=$X_{5'}$=H
3Cl-BT-es: X_5=$X_{5'}$=Cl, $X_{3'}$=X_4=$X_{4'}$=H
3Cl-BT-et: $X_{4'}$=X_5=Cl, $X_{3'}$=X_4=$X_{5'}$=H

3Cl-BT-eu: $X_{3'}$=X_5=Cl, X_3=$X_{4'}$=$X_{5'}$=H
3Cl-BT-ev: X_3=$X_{3'}$=Cl, $X_{4'}$=X_5=$X_{5'}$=H
3Cl-BT-ew: X_3=$X_{4'}$=Cl, $X_{3'}$=X_5=$X_{5'}$=H
3Cl-BT-ex: $X_{3'}$=$X_{5'}$=Cl, X_3=$X_{4'}$=X_5=H
3Cl-BT-ey: $X_{3'}$=X_5=Cl, $X_{3'}$=$X_{4'}$=$X_{5'}$=H
3Cl-BT-ez: $X_{4'}$=X_5=Cl, X_3=$X_{3'}$=$X_{5'}$=H
3Cl-BT-eA: X_5=$X_{5'}$=Cl, X_3=$X_{3'}$=$X_{4'}$=H
3Cl-BT-eB: X_3=$X_{4'}$=Cl, $X_{3'}$=X_5=$X_{5'}$=H
3Cl-BT-eC: X_3=$X_{5'}$=Cl, $X_{3'}$=$X_{4'}$=X_5=H
3Cl-BT-eD: $X_{4'}$=X_5=Cl, X_3=$X_{3'}$=X_5=H

4Cl-BT-ea: X_4=$X_{4'}$=$X_{5'}$=Cl, X_3=$X_{3'}$=H
4Cl-BT-eb: $X_{3'}$=$X_{4'}$=$X_{5'}$=Cl, X_3=X_4=H
4Cl-BT-ec: $X_{3'}$=X_4=$X_{5'}$=Cl, X_3=$X_{4'}$=H
4Cl-BT-ed: $X_{3'}$=X_4=$X_{4'}$=Cl, X_3=$X_{5'}$=H
4Cl-BT-ee: X_3=$X_{3'}$=X_4=Cl, $X_{4'}$=$X_{5'}$=H
4Cl-BT-ef: X_3=X_4=$X_{5'}$=Cl, $X_{3'}$=$X_{4'}$=H
4Cl-BT-eg: X_3=X_4=$X_{4'}$=Cl, $X_{3'}$=$X_{5'}$=H
4Cl-BT-eh: X_3=$X_{3'}$=$X_{5'}$=Cl, X_4=$X_{4'}$=H
4Cl-BT-ei: X_3=$X_{3'}$=$X_{4'}$=Cl, X_4=$X_{5'}$=H
4Cl-BT-ej: X_3=$X_{4'}$=$X_{5'}$=Cl, $X_{3'}$=X_4=H

4Cl-BT-ek: $X_{3'}$=X_4=$X_{5'}$=Cl, $X_{4'}$=X_5=H
4Cl-BT-el: $X_{3'}$=$X_{4'}$=$X_{5'}$=Cl, X_4=X_5=H
4Cl-BT-em: $X_{3'}$=X_4=$X_{4'}$=Cl, X_5=$X_{5'}$=H
4Cl-BT-en: $X_{3'}$=X_4=X_5=Cl, $X_{4'}$=$X_{5'}$=H
4Cl-BT-eo: $X_{3'}$=X_5=$X_{5'}$=Cl, X_4=$X_{4'}$=H
4Cl-BT-ep: $X_{3'}$=$X_{4'}$=X_5=Cl, X_4=$X_{5'}$=H
4Cl-BT-eq: X_4=$X_{4'}$=$X_{5'}$=Cl, $X_{3'}$=X_5=H
4Cl-BT-er: X_4=X_5=$X_{5'}$=Cl, $X_{3'}$=$X_{4'}$=H
4Cl-BT-es: $X_{4'}$=X_5=$X_{5'}$=Cl, $X_{3'}$=X_4=H
4Cl-BT-et: X_4=$X_{4'}$=X_5=Cl, $X_{3'}$=$X_{5'}$=H

4Cl-BT-eu: $X_{3'}$=$X_{3'}$=X_5=Cl, $X_{4'}$=$X_{5'}$=H
4Cl-BT-ev: $X_{3'}$=$X_{4'}$=X_5=Cl, $X_{3'}$=$X_{5'}$=H
4Cl-BT-ew: $X_{3'}$=X_5=$X_{5'}$=Cl, $X_{3'}$=$X_{4'}$=H
4Cl-BT-ex: $X_{3'}$=$X_{3'}$=$X_{4'}$=Cl, X_5=$X_{5'}$=H
4Cl-BT-ey: $X_{3'}$=$X_{3'}$=X_5=Cl, $X_{4'}$=$X_{5'}$=H
4Cl-BT-ez: $X_{3'}$=$X_{4'}$=X_5=Cl, $X_{3'}$=$X_{5'}$=H
4Cl-BT-eA: $X_{3'}$=$X_{4'}$=$X_{5'}$=Cl, $X_{3'}$=X_5=H
4Cl-BT-eB: $X_{3'}$=X_5=$X_{5'}$=Cl, $X_{3'}$=$X_{4'}$=H
4Cl-BT-eC: $X_{4'}$=X_5=$X_{5'}$=Cl, $X_{3'}$=$X_{3'}$=H
4Cl-BT-eD: $X_{3'}$=$X_{4'}$=X_5=Cl, $X_{3'}$=X_5=H

5Cl-BT-ea: $X_{3'}$=X_4=$X_{4'}$=$X_{5'}$=Cl, X_3=H
5Cl-BT-eb: X_3=X_4=$X_{4'}$=$X_{5'}$=Cl, $X_{3'}$=H
5Cl-BT-ec: X_3=$X_{3'}$=X_4=$X_{4'}$=Cl, $X_{5'}$=H
5Cl-BT-ed: X_3=$X_{3'}$=X_4=$X_{5'}$=Cl, $X_{4'}$=H
5Cl-BT-ee: X_3=$X_{3'}$=$X_{4'}$=$X_{5'}$=Cl, X_4=H

5Cl-BT-ef: $X_{3'}$=X_4=$X_{4'}$=X_5=Cl, $X_{5'}$=H
5Cl-BT-eg: $X_{3'}$=X_4=X_5=$X_{5'}$=Cl, $X_{4'}$=H
5Cl-BT-eh: $X_{3'}$=X_4=$X_{4'}$=X_5=Cl, $X_{5'}$=H
5Cl-BT-ei: $X_{3'}$=$X_{4'}$=X_5=$X_{5'}$=Cl, X_4=H
5Cl-BT-ej: X_4=$X_{4'}$=X_5=$X_{5'}$=Cl, $X_{3'}$=H

5Cl-BT-ek: X_3=$X_{3'}$=X_5=$X_{5'}$=Cl, $X_{4'}$=H
5Cl-BT-el: X_3=$X_{3'}$=$X_{4'}$=X_5=Cl, $X_{5'}$=H
5Cl-BT-em: X_3=$X_{4'}$=X_5=$X_{5'}$=Cl, $X_{3'}$=H
5Cl-BT-en: X_3=$X_{4'}$=X_5=$X_{5'}$=Cl, $X_{3'}$=H
5Cl-BT-eo: X_3=$X_{3'}$=$X_{4'}$=X_5=Cl, X_5=H

Figure 1. Relative potential energy levels of all possible geometric structures of the neutral derivatives and π-complexes including atomic charges (NBO, au) and geometric parameters calculated at the MP2/6-311+G** level. The units of the relative potential energy (ΔE), length (r), and dihedral angle (ϕ: S–C_2–C_2–S torsion angle) are electron volt (eV), angstrom (Å), and degree, respectively. 5,5′-Dichlorinated, 3,3′-dichlorinated, and 4,4′-dichlorinated π-complexes are denoted as **P**, **Q**, and **R**, respectively. The relative potential energy of the reactants (bithiophene derivatives and chlorine cation) in each step is set to zero and indicated as solid line. The relative energy between π-complex and the reactant is defined as the relative vertical energy.

chlorination step were similar to those at the fifth step. The energy gaps between two groups were much larger than the gaps within any single group. Because the lowest transition energy, the transition π-complexes of the **P** group could be primarily formed. The **P** structures were more planar ($\phi \approx 0$ or 180 degrees) than those of **R**. The lengths of $r_{C2-C2'} \approx 1.400$–1.420 Å in **P** were shorter than those of **R** ($r \approx 1.445$ Å). The $r_{C2-C2'}$ lengths of the transition bithiophene derivatives are slightly longer than that of benzene ($r_{cc} = 1.39$ Å) and shorter than that of ethane. Therefore, the structures of **P** had the π-conjugation along the bithiophene frame. And the **P** group in the transition π-complexes was the most stable. The relative activation energies of the bromination of bithiophene using molecular orbital calculations were investigated by Kellogg et al.[15] The relative energy at the 5,5′-positions is lower than those at the other position. The regioselective synthesis[4,16,17] for the halogenations on bithiophenes were in good agreement with our results.

To investigate the regioselectivity dependence on atomic charges, the ($Cl^+ \cdots C_5^{\delta-}$) interactions between a chlorine and the 5-carbon of **Cl-BT-a** and **Cl-BT-b** and the HOMO–LUMO gaps of **2Cl-BT-ea** and **2Cl-BT-eb** are represented in Figure 2. In the chlorination step of **Cl-BT-a** and **Cl-BT-b**, a chlorine could preferentially approach the 5-carbon with the most negative atomic charge ($q_{C5} = -0.381$ au for **Cl-BT-a** and $q_{C5} = -0.404$ au for **Cl-BT-b**). The transition π-complexes of **2Cl-BT-ea** and **2Cl-BT-eb** were primarily formed via ($Cl^+ \cdots C_5^{\delta-}$) interactions. As shown in Figure 2a, the more stable **2Cl-BT-ea** π-complex was produced from **Cl-BT-b** with the more negative charge ($q_{C5} = -0.404$ au) on C_5, while the unstable **2Cl-BT-eb** π-complex was produced from **Cl-BT-a** with the less negative charge. The ($Cl^+ \cdots C_5^{\delta-}$) interaction between Cl^+ and C_5 on **Cl-BT-b** might be stronger than that between Cl^+ and C_5 on **Cl-BT-a**. Due to the stronger ($Cl^+ \cdots C_5^{\delta-}$) interaction, the relative energy of **2Cl-BT-ea** was more stable than **2Cl-BT-eb**. Because the HOMO–LUMO gap ($\Delta E_{H-L} = 8.65$ eV) of **2Cl-BT-ea** was larger than that ($\Delta E_{H-L} = 8.45$ eV) of **2Cl-BT-eb** (Figure 2b), the HOMO level of **2Cl-BT-ea** was lower than that of **2Cl-BT-eb**. Therefore, the lower HOMO level of **2Cl-BT-ea** corresponds to that of **Cl-BT-b** and **2Cl-BT-ea** was more stable than **2Cl-BT-eb**. As a result, the negative atomic charge of the carbon on bithiophene derivatives is an important factor to determine the specific position in the selective chlorination.

To check the reactivity in each chlorination step, the ($Cl^+ \cdots C_5^{\delta-}$) interaction between a chlorine cation and the most

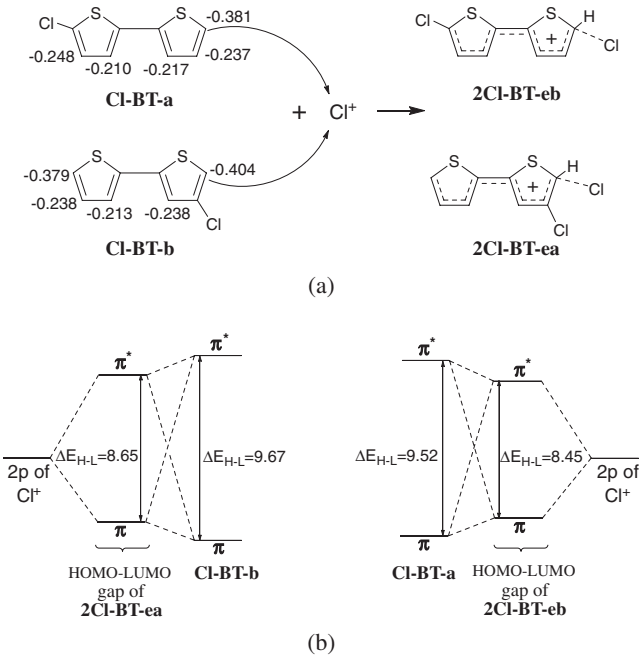

Figure 2. (a) The ($Cl^{+}\cdots C_5^{\delta-}$) interactions between a chlorine cation and the largely negative 5-carbons of **Cl-BT-a** and **Cl-BT-b**. (b) Relative HOMO–LUMO energy gaps (ΔE_{H-L}, eV) of **2Cl-BT-ea** and **2Cl-BT-eb** produced from the ($Cl^{+}\cdots C_5^{\delta-}$) interactions.

negative 5-carbons from **BT** to **5Cl-BT-c** are drawn in Figure 3. The atomic charges of the 5,5′-carbons on neutral derivatives had relatively large negative values ($q_{C5} = -0.404 - -0.354$ au), and the charges were more negative than those of the 3,3′- and 4,4′-carbons (Figure 1). The 5,5′-carbons located outside of the ring and a chlorine could easily approach the 5,5′-positions without any steric hindrance. Because of the most negative atomic charges (from $q_{C5} = -0.385$ au for **BT** to $q_{C5} = -0.372$ au for **5Cl-BT-c**) on the 5-carbon, a chlorine could interact with the 5-carbon more readily than with the other 3,3′- and 4,4′-carbons (and the other 5-carbon with the second and third negative charges). In each chlorinated step, the most stable transition π-complexes were also formed from the strongest ($Cl^{+}\cdots C_5^{\delta-}$) interaction between Cl^{+} and C_5. That is, all sequential chlorinations preferentially occurred at 5,5′-positions with the most negative atomic charges. Therefore, the Cl–C_5 bond at the 5-position might be stronger than those at the other positions. As a result, the relative transition energy levels of the transition 5-chlorinated π-complexes were lower than the other π-complexes.

To compare the relative stability of the **Cl-BT-ea** π-complex with (Cl–C_5) and **Cl-BT-eb** π-complex with (Cl–C_3), the HOMO–LUMO energy diagram and the geometric structures of the transition π-complexes are represented in Figure 4. Because the atomic charges of the 5,5′-carbons on neutral derivatives were more negative than those of the 3,3′-carbons, the ($Cl^{+}\cdots C_5^{\delta-}$) interaction might be stronger than that of ($Cl^{+}\cdots C_3^{\delta-}$) (Figure 4a). The HOMO–LUMO gap ($\Delta E_{H-L} = 8.78$ eV) of **Cl-BT-ea** with (Cl–C_5) was larger than that ($\Delta E_{H-L} = 8.03$ eV) of **Cl-BT-eb** with (Cl–C_3). Thus, the HOMO level of **Cl-BT-ea** was lower than that of **Cl-BT-eb**.

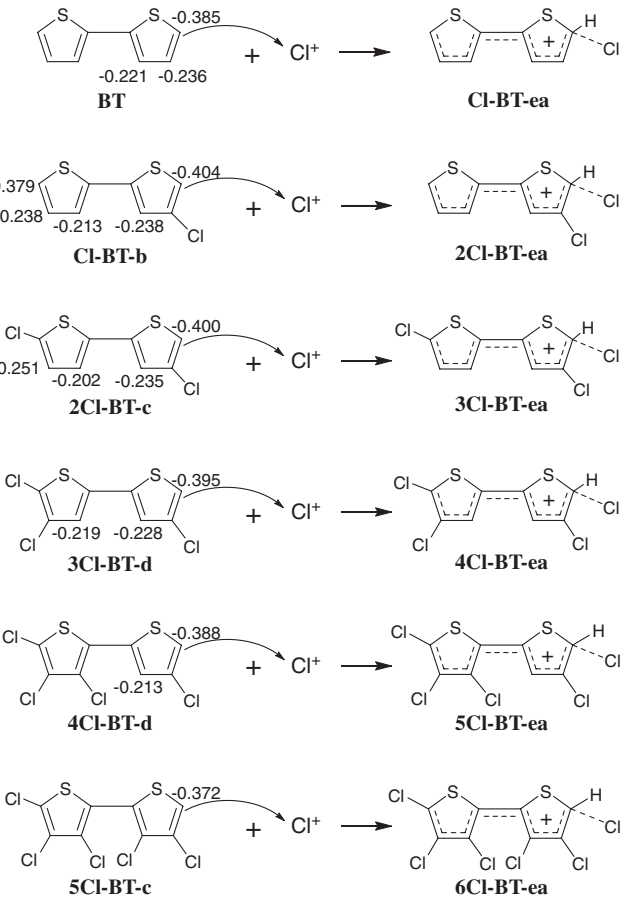

Figure 3. Diagram showing the most strong ($Cl^{+}\cdots C_5^{\delta-}$) interaction between a chlorine cation and the most negative 5-carbon from **BT** to **5Cl-BT-c**.

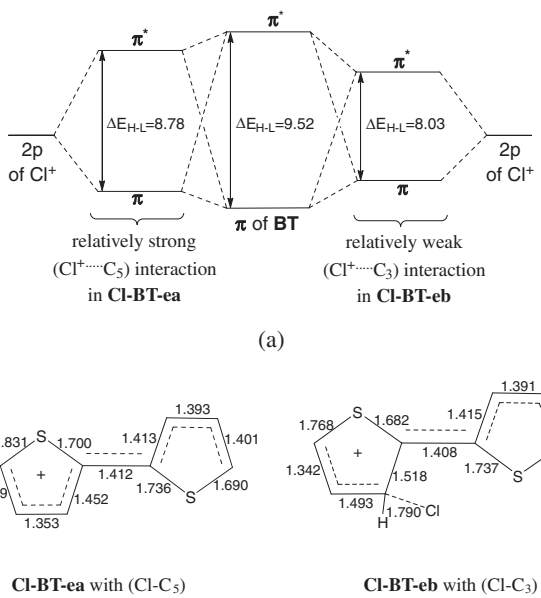

Figure 4. (a) Relative HOMO–LUMO energy gaps (ΔE_{H-L}, eV) and structures (b) of **Cl-BT-ea** with (Cl–C_5) and **Cl-BT-eb** with (Cl–C_3) optimized at the MP2/6-311+G** level.

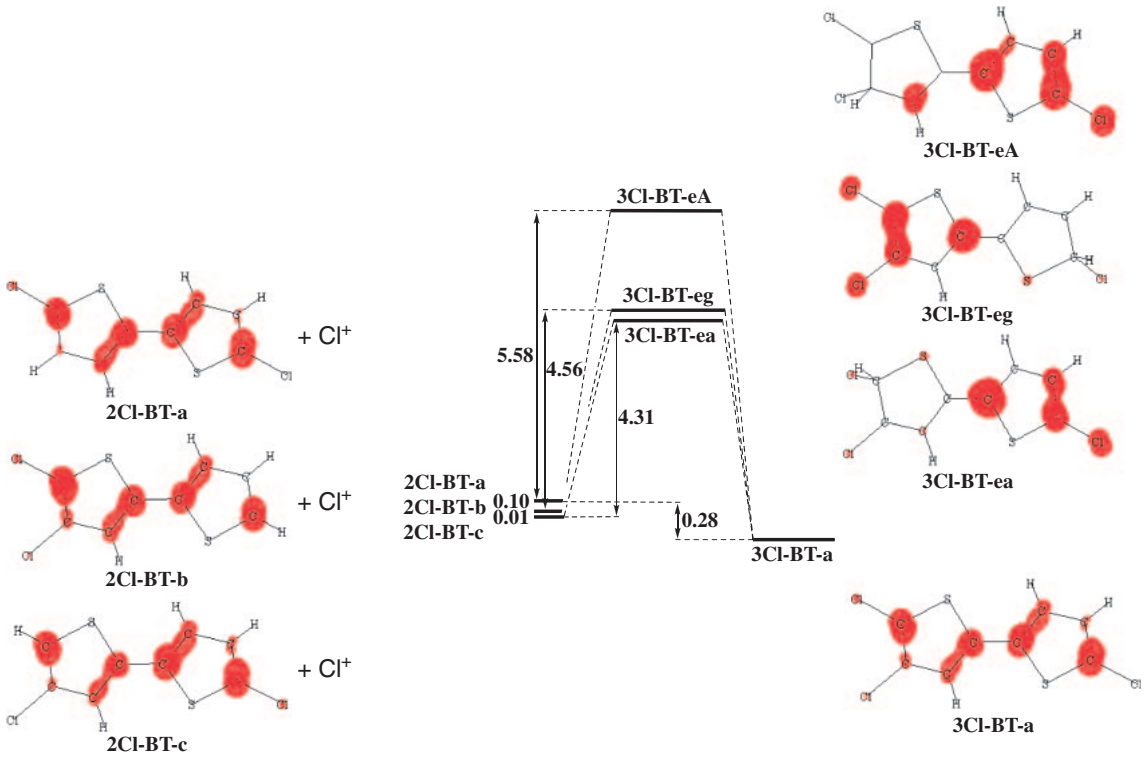

Figure 5. The relative energy levels (eV) and HOMO orbitals of the reactants, π-complexes, and products from **2Cl-BT** to **3Cl-BT-a** optimized at the MP2/6-311+G** level.

As a result, the structure of **Cl-BT-ea** was more stable than that of **Cl-BT-eb**. As shown in Figure 4b, all C–C lengths in **Cl-BT-ea** were slightly shorter than that of the single C–C bond and longer than that of the double C=C bond. Thus, the π-conjugation along the bithiophene frame was connected. Meanwhile, since the (C_2–C_3) length ($r_{C2\text{–}C3} \approx 1.518$ Å) in **Cl-BT-eb** was similar to the normal C–C length of ethane, the π-conjugation between C_2 and C_3 was very weak. The length ($r_{Cl\text{–}C5} \approx 1.770$ Å) of the Cl–C_5 bond was longer than that ($r_{Cl\text{–}C3} \approx 1.790$ Å) of Cl–C_3. The Cl–C_5 bond was stronger than the Cl–C_3 bond. As a result, due to the stable electronic distribution along the bithiophene frame in **Cl-BT-ea**, the relative energy level of the transition 5-chlorinated π-complexes was lower and more stable. And the ($Cl^{+}\cdots C_5^{\delta-}$) interaction proceeded to be favored energetically and geometrically.

The more detailed energy levels and HOMO orbitals of the reactants, transition π-complexes, and products from **2Cl-BT** to **3Cl-BT-a** optimized at the MP2/6-311+G** level are presented in Figure 5. The contribution of the HOMO at the 2,2′-, 3,3′-, and 5,5′-carbons of the reactants (**2Cl-BT-a**, **2Cl-BT-b**, and **2Cl-BT-c**) and product (**3Cl-BT-a**) were relatively large. A chlorine cation can easily approach to the 5,5′-positions with large HOMO lobe and it can strongly interacts with the 5,5′-carbons than the other positions. Meanwhile, due to the new (Cl–C) bond in the transition π-complexes (**2Cl-BT-ea**, **2Cl-BT-eg**, and **2Cl-BT-eA**), the HOMO lobe at the 5,5′-carbons of the reactive center disappeared. **3Cl-BT-a** can be produced by the chlorination as three reaction paths, namely on the 4-carbons (very small lobe) of **2Cl-BT-a** ($q_{C4} = -0.249$ au) via **3Cl-BT-eA** ($\Delta E_{transition} = 5.58$ eV), on the 5′-carbons (large lobe) of **2Cl-BT-b** ($q_{C5'} = -0.376$ au) via **3Cl-BT-eg** ($\Delta E_{transition} = 0.10 + 4.20 + 0.11 + 0.03 + 0.01 + 0.04 + 0.07 = 4.56$ eV), and on the 5′-carbons (large lobe) of **2Cl-BT-c** ($q_{C5'} = -0.400$ au) via **3Cl-BT-ea** ($\Delta E_{transition} = 0.10 + 0.01 + 4.20 = 4.31$ eV). Meanwhile, since the gaps of the relative potential energy in the **P** group are small, the various bithiophene products in the chlorination step can be produced. From the experimental results, various product isomers including the by-products were simultaneously observed under the same conditions. Therefore, each isomer (main and by-products) as the reactant are used to produce the corresponding products in the sequential chlorination.

As indicated in Figure 1, a **Cl-BT-ea** with the lowest transition energy ($\Delta E_1 = 4.31$ eV) was formed by preferential chlorination at the 5-carbon of **BT**. Although the atomic charge ($q_{C5} = -0.404$ au) of 5-carbon in **Cl-BT-b** was the most negative, the transition energy ($\Delta E_{transition} = 4.28 + 0.02 = 4.30$ eV) of **2Cl-BT-eb** was smaller than those of the other isomers. Finally, the **2Cl-BT-a** product was formed via the energetically favorable **2Cl-BT-eb**. By the continuous third and fourth chlorinations on the bithiophenes, **3Cl-BT-ea** ($\Delta E_{transition} = 0.10 + 0.01 + 4.20 = 4.31$ eV) and **4Cl-BT-ea** ($\Delta E_{transition} = 0.03 + 0.05 + 0.02 + 4.33 = 4.43$ eV) were produced by the chlorinations on the 5-carbons of **2Cl-BT-c** ($q_{C5} = -0.400$ au) and **3Cl-BT-d** ($q_{C5} = -0.395$ au), respectively (Figure 3). Due to the lower transition barrier for the chlorination at the 5,5′-carbon, the neutral 5,5′-chlorinated bithiophenes can be formed via their energetically stable π-complexes. In previous synthetic methods,[15–17] the derivatives from 5-chlorobithiophene to 3,3′,5,5′-tetrachlorobithiophene were synthesized subsequently and selectively. The 5,5′-

dichlorinated derivatives were a major product. After the 5,5′-positions were substituted, the 3,3′-substituted derivatives were produced. In our optimized structures from **BT** to **3Cl-BT**, the electrophilic chlorination of bithiophene derivatives were kinetically dependent on relative potential energy level ($\Delta E_{transition}$) of the π-complexes. Our results are consistent with previous theoretical[7–9,26–30] and experimental[10–19,31,32] results. In particular, the ratios of the experimental yield[15–17] between 5,5′- and 3,3′-substituted derivatives were similar to the relative stability of our optimized bithiophene derivatives.

In the fifth and sixth chlorinations, **5Cl-BT-ea** and **6Cl-BT-ea** were formed by the interaction between a chlorine and the 5-carbons (Figure 3). The transition energies of **5Cl-BT-ea** and **6Cl-BT-ea** were much higher than those in the previous chlorination steps. Due to the higher transition energies {4.87 (=0.02 + 0.03 + 0.06 + 4.76) eV for **5Cl-BT-ea**, 5.08 (=0.11 + 0.08 + 4.89) eV for **6Cl-BT-ea**}, the penta- and hexachlorobithiophenes could not be easily formed. Although penta- and hexachlorobithiophenes have been observed in previous studies,[18,19] it was difficult to synthesize these two bithiophenes under the mild conditions. In recently proposed synthetic methods,[15–17] penta- and hexachlorobithiophenes were not synthesized. Consequently, the electrophilic chlorinations from **BT** to **6Cl-BT** were depended primarily by the relative transition energy level of the π-complexes. As shown in Scheme 1, the relative potential energy levels (ΔE_4 and ΔE_{10} for the neutral, ΔE_1 and ΔE_7 for the π-complex) of the 5,5′-dichlorinated neutral and transition derivatives were the highest and lowest, respectively. In each chlorination step, the calculated transition energies ($\Delta E_{transition} = 4.30$–$5.08$ eV) for the 5,5′-dichlorinated π-complexes were smallest. Therefore, our computational results were well consistent with the sequential selectivity for the specific 5,5′-carbons.

From **BT** to **6Cl-BT**, the products of all bithiophene derivatives were dependent on its relative potential energies of the transition π-complexes. In the neutral derivatives, the average values of the atomic charges at the 5,5′-positions were the most negative. By the strong ($Cl^{+}\cdots C_5^{\delta-}$) interactions between Cl^+ and C_5, the transition π-complexes in each chlorination step were primarily formed. In the sequential chlorination reaction, the substitution reaction of halogen to 2,2′-bithiophene is energetically favored at 5,5′-positions adjacent to sulfur atom compared to 3,3′- and 4,4′-positions. With increasing Cl, the steric hindrance on the derivatives increases stepwise. Because the 5,5′-carbons are located outside of the ring, the chlorination at the 5,5′-positions can be easily occurred. After the 5,5′-positions were substituted, the 3,3′- or 4,4′-positions at C farthest from S were changed. As a result, our results were in well agreement with the previous synthetic results (the isolated yields (%) of isomers are depended on the reaction conditions).[15–17]

As shown in Figure 6, four (**d**, **e**, **f**, and **g**) resonant structures of 5′-chlorination and four (**i**, **j**, **k**, and **l**) resonant structures of 3′-chlorination show double bond character in the C_2–$C_{2'}$ bond. From the double bond character of these π-complexes, the π-conjugation between two rings in the eight resonant structures (**d**, **e**, **f**, **g**, **i**, **j**, **k**, and **l**) could be formed. Due to the π-conjugation (delocalization energy), the C_2–$C_{2'}$ bond and the dihedral angle between two rings become short and planar, respectively. The stronger π-conjugation was associated with shorter $r_{C2-C2'}$ length. Therefore, **P** and **Q** were more stable. Meanwhile, in the chlorination at the 5′-, 3′-, and 4′-positions of **Cl-BT-a**, the 7, 5, and 2 resonant structures of the 5,5′-, 5,3′-, and 5,4′-dichlorinated π-complexes can be drawn, respectively. The 5,5′-dichlorinated π-complexes (**P**) can have more associated resonant structures than those chlorinated at 3,3′- and 4,4′-carbons. By the number of the resonant structures, **P** was the most stable. As a result, the chlorination reaction on the bithiophenes proceeded to be energetically and sterically favored at the specific 5,5′-positions. As discussed by Joule et al.,[24] the positional selectivity for electrophilic substitution on thiophene is influenced by the delocalization of the electron density. As illustrated in Figure 6, the length of the C_2–$C_{2'}$ bond was closely related to the dihedral angle between two rings. In the transition π-complexes, the structural delocalization formed by the π-conjugations and the extent of the overlap between the p_z-orbitals played an important role in the relative energy and in the geometric structures. The relative energy levels of the π-complexes determined the selectivity of the chlorination reactions.

As shown in Figure 1, the 3,3′-carbons in the neutral bithiophenes held the smallest atomic charge in the thiophene ring ($q \approx -0.21$ au). The 3,3′-carbons locate between two rings. When a chlorine interacts with a 3-carbon, slight steric hindrance can occur from the neighboring ring. In the 3,3′-dichlorinated π-complexes, the dihedral angles were approximately $\phi \approx 0$ or 180 degrees and the π-conjugation between two rings formed well. Due to repulsion of (Cl···Cl) in the π-complexes, the structures of the **Q** group were optimized to be *anti*. The relative potential levels were more unstable. In the 4,4′-carbons of neutral derivatives, the atomic charges ($q \approx -0.24$ au) were more negative than those of the 3,3′-carbons. Because the 4,4′-carbons are located outside of the ring, they can be readily approached by a chlorine without steric hindrance. In the transition π-complexes, the **R** group displayed the highest transition energy. The optimized structures of **R** did not show planar geometry with $\phi \approx 130$–165 degrees. The length of $r_{C2-C2'}$ (≈ 1.44 Å) was the longest. As shown in Figure 6, two resonant structures in the 4′-chlorination can only be drawn. Due to the long C_2–$C_{2'}$ bond and the nonplanar structure, π-conjugation between two rings was not formed. As a result, the **R** group was the most unstable.

The selective chlorinations on the bithiophene derivatives could be accomplished by controlling factors in relation to the relative stability of the chlorinated transition π-complexes. That is, *the selective chlorinations were controlled by a kinetically reactive mechanism*. The factors were the atomic charges, the positions of the substituted chlorine, the structures ($R_{C2-C2'}$, ϕ) of the transition π-complexes, and the π-conjugation (delocalization energy). The order of selective reactivity was 5,5′-dichlorinated > 3,3′-dichlorinated > 4,4′-dichlorinated derivatives. Although the electrophilic substitution reactions in the multichloroheterocycles are complex, the synthesis of the conjugated polymers could be controlled by selective substitution steps in relation to the relative transition energy levels (ΔE_1, ΔE_2, ΔE_3, ...) of the π-complexes.

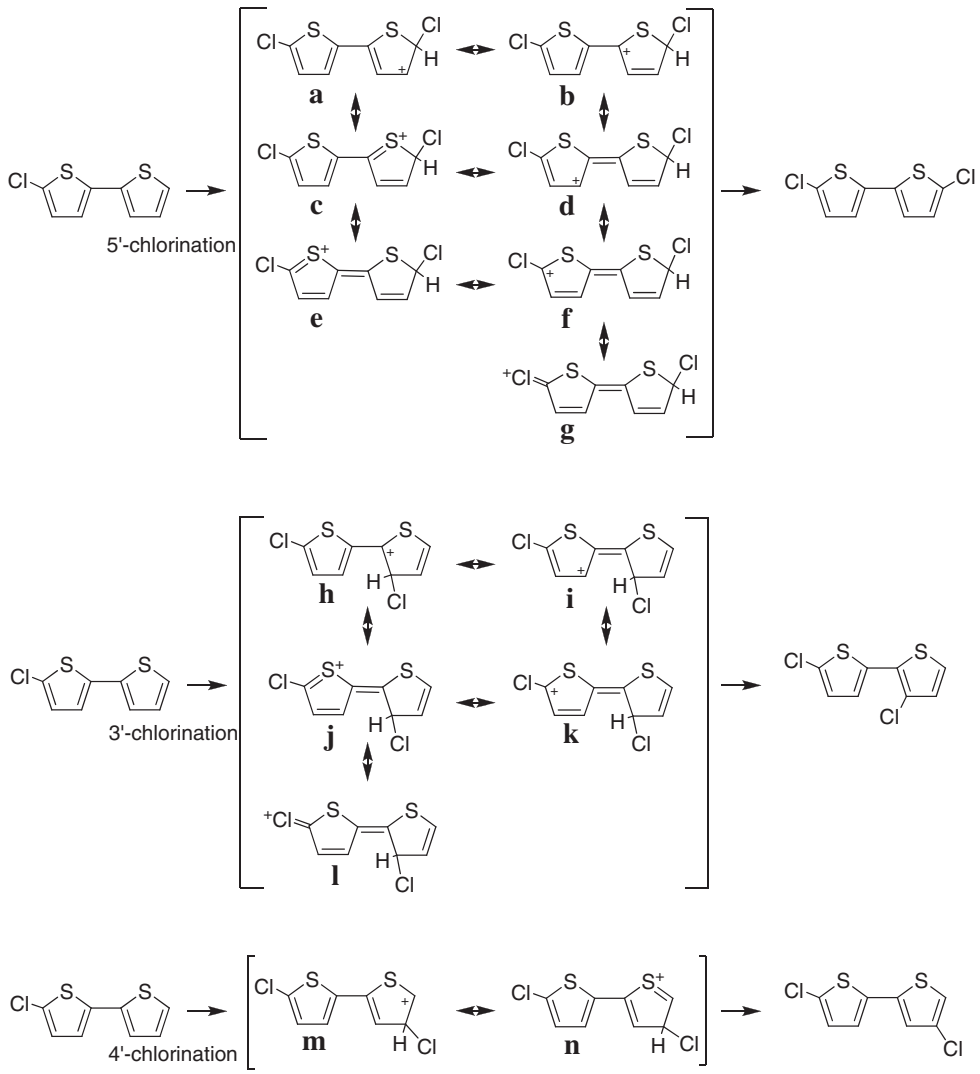

Figure 6. The resonant structures of the 5,5′-dichlorinated, 5,3′-dichlorinated, and 5,4′-dichlorinated π-complexes formed by the chlorination reaction at the 5′-, 3′-, and 4′-positions of **Cl-BT-a**.

Conclusion

We optimized the geometric structures of the equilibrium bithiophene derivatives and its transition π-complexes at the MP2/6-311+G** level and drew the relative energy diagrams for the structures. From **BT** to **6Cl-BT**, the 5,5′-dichlorinated neutral isomers (the more chlorinated at the C adjacent to the S) were less stable than 3,3′-dichlorinated (more chlorinated at C farthest from S). The pseudo-*anti* in less chlorinated derivatives was more stable. With increasing chlorine, the geometric structures optimized to vertical. In the π-complexes, the relative energy levels (ΔE_1, ΔE_7, ...) of 5,5′-dichlorinated π-complexes were the lowest. Due to the repulsion of (Cl···Cl) and the weak ($Cl^+ \cdots C_3^{\delta-}$) interaction, the relative energy levels (ΔE_2, ΔE_8, ...) of 3,3′-dichlorinated π-complexes were higher. Energetically, the higher potential levels (ΔE_4, ΔE_{10}, ...) of the 5,5′-dichlorinated neutrals contributed to the decrease of the transition energy level for the next chlorination. By the lowest transition energy of the 5,5′-substituted π-complexes, the selective chlorinations on the bithiophene derivatives easily occurred at the specific 5,5′-positions.

In each chlorination step, the transition π-complexes were primarily formed via the ($Cl^+ \cdots C_5^{\delta-}$) interactions. A chlorine could preferentially approach the 5-carbon with the most negative atomic charges. And the ($Cl^+ \cdots C_5^{\delta-}$) interaction between Cl^+ and C_5 formed subsequently. Due to the stronger ($Cl^+ \cdots C_5^{\delta-}$) interaction, the HOMO–LUMO gap increased and the relative transition energy level of the π-complexes was lower. From **Cl-BT-ea** to **6Cl-BT-ea**, the relative transition energy levels were lower than those of the other π-complexes. In the 3,3′-dichlorinated π-complexes, the relative potential levels were less stable than that of the 3,3′-dichlorinated π-complexes via the repulsion of (Cl···Cl). In the 4,4′-dichlorinated π-complexes without the π-conjugation, the relative energy level was the most unstable. We found that the order of selective reactivity was 5,5′-dichlorinated > 3,3′-dichlorinated > 4,4′-dichlorinated derivatives. Consequently, the regioselective chlorinations from **BT** to **6Cl-BT** were dependent primarily by the relative energy gaps (ΔE_1, ΔE_2, ΔE_3, ...) of the π-complexes. The relative stability of the specific π-complexes was primarily related to the atomic charges of the carbon atom, the position and number of substituted chlorine,

the structures ($R_{C2-C2'}$, ϕ, steric hindrance, repulsion) of the neutral and transition derivatives, and the π-conjugation (these were the factors of the driving force for the regioselectivity).

We gratefully acknowledge the support of the Chemistry Research Fund of Gyeongsang National University. This work was supported by the fund of Research Promotion Program (RPP-2010-018), Gyeongsang National University.

References

1 J. Roncali, *Chem. Rev.* **1992**, *92*, 711.
2 M. Funahashi, J.-I. Hanna, *Adv. Mater.* **2005**, *17*, 594.
3 S. Zrig, G. Koeckelberghs, T. Verbiest, B. Andrioletti, E. Rose, A. Persoons, I. Asselberghs, K. Clays, *J. Org. Chem.* **2007**, *72*, 5855.
4 Y. Zhu, I. Heim, B. Tieke, *Macromol. Chem. Phys.* **2006**, *207*, 2206.
5 Y.-L. Liu, J.-K. Feng, A.-M. Ren, *J. Comput. Chem.* **2007**, *28*, 2500.
6 S. K. Min, E. C. Lee, H. M. Lee, D. Y. Kim, D. Kim, K. S. Kim, *J. Comput. Chem.* **2008**, *29*, 1208.
7 N. DiCésare, M. Belletête, F. Raymond, M. Leclerc, G. Durocher, *J. Phys. Chem. A* **1998**, *102*, 2700.
8 F. C. Grozema, P. Th. van Duijnen, Y. A. Berlin, M. A. Ratner, L. D. A. Siebbeles, *J. Phys. Chem. B* **2002**, *106*, 7791.
9 G. Raos, A. Famulari, S. V. Meille, M. C. Gallazzi, G. Allegra, *J. Phys. Chem. A* **2004**, *108*, 691.
10 J. P. Knowles, A. Whiting, *Org. Biomol. Chem.* **2007**, *5*, 31.
11 M. Takahashi, K. Masui, H. Sekiguchi, N. Kobayashi, A. Mori, M. Funahashi, N. Tamaoki, *J. Am. Chem. Soc.* **2006**, *128*, 10930.
12 K. Masui, H. Ikegami, A. Mori, *J. Am. Chem. Soc.* **2004**, *126*, 5074.
13 A. Krasovskiy, A. Tishkov, V. del Amo, H. Mayr, P. Knochel, *Angew. Chem., Int. Ed.* **2006**, *45*, 5010.
14 H. Tohma, M. Iwata, T. Maegawa, Y. Kiyono, A. Maruyama, Y. Kita, *Org. Biomol. Chem.* **2003**, *1*, 1647.
15 R. M. Kellogg, A. P. Schaap, H. Wynberg, *J. Org. Chem.* **1969**, *34*, 343.
16 T. Sone, Y. Abe, *Bull. Chem. Soc. Jpn.* **1973**, *46*, 3603.
17 K.-J. Jung, S. B. Kang, J.-E. Won, S.-E. Park, K. H. Park, J. K. Park, S.-G. Lee, Y.-J. Yoon, *Synlett* **2009**, 490.
18 K. Yui, Y. Aso, T. Otsubo, F. Ogura, *Bull. Chem. Soc. Jpn.* **1989**, *62*, 1539.
19 A. G. Mack, H. Suschitzky, B. J. Wakefield, *J. Chem. Soc., Perkin Trans. 1* **1980**, 1682.
20 C. Y. Legault, Y. Garcia, C. A. Merlic, K. N. Houk, *J. Am. Chem. Soc.* **2007**, *129*, 12664.
21 Y. Garcia, F. Schoenebeck, C. Y. Legault, C. A. Merlic, K. N. Houk, *J. Am. Chem. Soc.* **2009**, *131*, 6632.
22 R. M. Souto Maior, K. Hinkelmann, H. Eckert, F. Wudl, *Macromolecules* **1990**, *23*, 1268.
23 S. T. Handy, Y. Zhang, *Chem. Commun.* **2006**, 299.
24 J. A. Joule, K. Mills, G. F. Smith, *Heterocyclic Chemistry*, 3rd ed., Chapman & Hall, London, **1996**, p. 225.
25 M. J. Frisch, G. W. Trucks, H. B. Schlegel, G. E. Scuseria, M. A. Robb, J. R. Cheeseman, J. A. Montgomery, Jr., T. Vreven, K. N. Kudin, J. C. Burant, J. M. Millam, S. S. Iyengar, J. Tomasi, V. Barone, B. Mennucci, M. Cossi, G. Scalmani, N. Rega, G. A. Petersson, H. Nakatsuji, M. Hada, M. Ehara, K. Toyota, R. Fukuda, J. Hasegawa, M. Ishida, T. Nakajima, Y. Honda, O. Kitao, H. Nakai, M. Klene, X. Li, J. E. Knox, H. P. Hratchian, J. B. Cross, C. Adamo, J. Jaramillo, R. Gomperts, R. E. Stratmann, O. Yazyev, A. J. Austin, R. Cammi, C. Pomelli, J. W. Ochterski, P. Y. Ayala, K. Morokuma, G. A. Voth, P. Salvador, J. J. Dannenberg, V. G. Zakrzewski, S. Dapprich, A. D. Daniels, M. C. Strain, O. Farkas, D. K. Malick, A. D. Rabuck, K. Raghavachari, J. B. Foresman, J. V. Ortiz, Q. Cui, A. G. Baboul, S. Clifford, J. Cioslowski, B. B. Stefanov, G. Liu, A. Liashenko, P. Piskorz, I. Komaromi, R. L. Martin, D. J. Fox, T. Keith, M. A. Al-Laham, C. Y. Peng, A. Nanayakkara, M. Challacombe, P. M. W. Gill, B. Johnson, W. Chen, M. W. Wong, C. Gonzalez, J. A. Pople, *Gaussian 03, Revision B.02*, Gaussian, Inc., Pittsburgh PA, **2003**.
26 G. Raos, A. Famulari, V. Marcon, *Chem. Phys. Lett.* **2003**, *379*, 364.
27 M. Concistré, L. D. Lorenzo, G. D. Luca, M. Longeri, G. Pileio, G. Raos, *J. Phys. Chem. A* **2005**, *109*, 9953.
28 E. Orti, P. M. Viruela, J. Sanchez-Marin, F. Tomas, *J. Phys. Chem.* **1995**, *99*, 4955.
29 N. D. Césare, M. Belletête, M. Leclerc, G. Durocher, *Synth. Met.* **1998**, *94*, 291.
30 J. Zhao, P. Li, Y. Li, Z. Huang, *THEOCHEM* **2007**, *808*, 125.
31 S. Samdal, E. J. Samuelsen, H. V. Volden, *Synth. Met.* **1993**, *59*, 259.
32 G. J. Pyrka, Q. Fernando, M. B. Inoue, M. Inoue, E. F. Velazquez, *Acta Crystallogr., Sect. C* **1988**, *44*, 562.
33 V. Bethmont, A. E. Kassmi, F. Fache, M. Lemaire, *Synth. Met.* **1998**, *93*, 197.